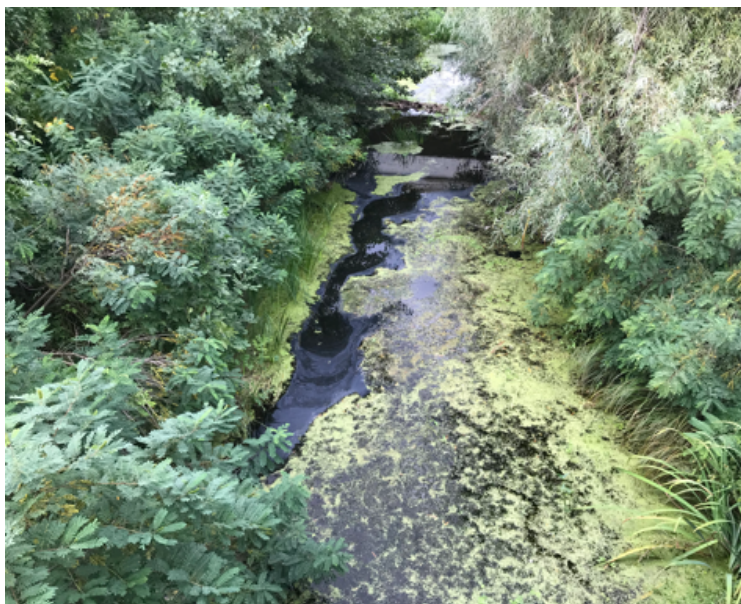


FINAL REPORT

ASSESSING SUSCEPTIBILITY OF RIVERS TO EUTROPHICATION USING REMOTE SENSING AND CATCHMENT MODELING (NNE 129990)



Lead Partner: Vera Istvánovics

ELKH-BME Water Research Group

31 March 2023, Budapest

TABLE OF CONTENTS

1. FIELD MEASUREMENTS.....	3
1.1. Stationary deployments.....	3
1.2. Snapshot measurements.....	5
2. MODELLING.....	7
2.1. Use of remote sensing in river water quality assessment.....	7
2.2. Application of the PhosFate-TAPIR model to the study rivers.....	12
2.3. Developing a simplified conceptual stream network eutrophication model.....	16
2.3.1. Methods.....	18
2.3.2. Results and Discussion.....	23
2.3.3. Conclusions.....	26
2.3.4. Miscellaneous.....	27
3. REFERENCES.....	27
4. APPENDIX 1.....	29
4.1. Response from the General Directorate of Water Management.....	29
4.2. Response from the ICPDR.....	30

The overarching aim of our project was to characterize vulnerability of rivers to eutrophication. Three types of approaches were combined: 1) field measurements of river water quality, 2) remote sensing and 3) catchment modelling. Chlorophyll *a* (Chl) data from field measurement campaigns were meant to qualitatively validate time averaged catchment-scale eutrophication models, whereas Chl timeseries extracted from past satellite imagery could be used both to calibrate and validate the models.

1. FIELD MEASUREMENTS

1.1. Stationary deployments

The original idea was to deploy an EXO2 multiparametric sonde (Yellow Springs Instruments, USA equipped with chlorophyll, phycocyanin, dissolved oxygen, turbidity, conductivity, pH, temperature and depth [pressure] sensors) near the mouth section of the study rivers. This plan had to be given up because it was very difficult to find safe deployment sites. Nevertheless, a relatively long deployment yielded unexpected and important results during late July 2020 in the Zala River at the outflow to the Kis-Balaton Reservoirs. A large flood wave passed while the device was continuously measuring water quality. Stage increased by 1 m on 25 July (Fig. 1). High turbidity (concentration of suspended solids), low concentration of dissolved oxygen and an increasing chlorophyll *a* concentration accompanied the ascending limb of the flood wave. The biomass increase could likely be attributed to flushing of the numerous nutrient-rich fishponds established on the tributaries of the Zala River (Honti et al., 2010). Concentration of dissolved oxygen dropped to 0-1 g m⁻³ and remained at this low level until the end of the deployment (29 July). The explanation is that heavy rains overloaded the

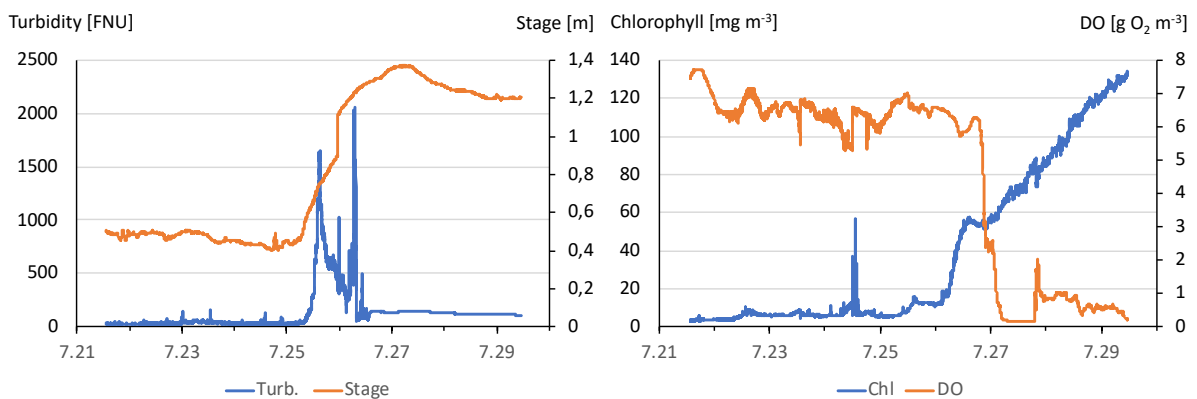


Figure 1: Turbidity and stage (left), concentration of chlorophyll *a* and dissolved oxygen (DO; right), in July 2020 in the Zala River above the Kis-Balaton Reservoirs.

sewers and wastewater treatment plants (WWTPs), which resulted in combined sewer overflows and activated the bypass mechanisms at WWTPs. This could transiently increase the nutrient loads to the Kis-Balaton manifold. Even particularly frequent traditional water quality monitoring may not detect such nutrient spills causing uncertainty in estimating nutrient retention efficiency of the Kis-Balaton Reservoirs. We recommend deploying autonomous water quality monitoring devices in river sections of special interest. These sections might, in a long run, include river inflows into important reservoirs, upstream sections of drinking water abstraction sites, downstream sections of large WWTPs, in- and outflow sections of large transboundary rivers.

Safe deployment was possible on the left shore of the Danube River in Budapest in July 2022 at the “Green Island” float (<http://www.tankerport.hu/index.php/en/>; 47.4813 N, 19.0590 E). Flow was low and decreased monotonically from $1800 \text{ m}^3 \text{ s}^{-1}$ to $1170 \text{ m}^3 \text{ s}^{-1}$. The EXO2 sonde was deployed at a depth of 2 m, that is about the middle of the water column. The concentration of chlorophyll *a* was low ($2\text{-}4 \text{ mg m}^{-3}$; Fig. 2) and oxygen saturation was sufficiently high (81-93%). Although several factors may contribute to low algal biomass, this observation is in harmony with our hypothesis that fluvial algae have meroplanktonic life history, that is they spend a significant fraction of their lifetime settled on the bottom (Istvánovics and Honti, 2011; Istvánovics et al., 2014) and this fraction is longer during low flow. A small but pronounced diel variability was clearly visible in both chlorophyll and dissolved oxygen (Fig. 2). Gross primary production averaged at $0.2 \text{ g O}_2 \text{ m}^{-2} \text{ d}^{-1}$; it was lower than the value ($\sim 1 \text{ g O}_2 \text{ m}^{-2} \text{ d}^{-1}$) estimated during the Joint Danube Survey 2 when both chlorophyll and discharge were somewhat higher than during our measurements (Dokulil and Qian, 2021).

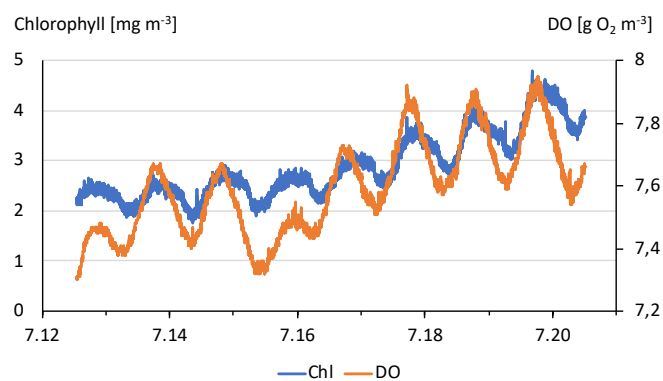


Figure 2: Concentration of chlorophyll *a* and dissolved oxygen (DO), in July 2022 in the Danube River in Budapest.

1.2. Snapshot measurements

Problems with stationary deployments led us to take snapshot water quality measurements at several sites along the study rivers. To capture network behavior, our strategy was to sample mouths of major tributaries and reservoirs/fishponds as well as the main river up- and downstream of those tributaries with the EXO2 sonde. The results are exemplified by the case of the Zagyva River network (Fig. 3).

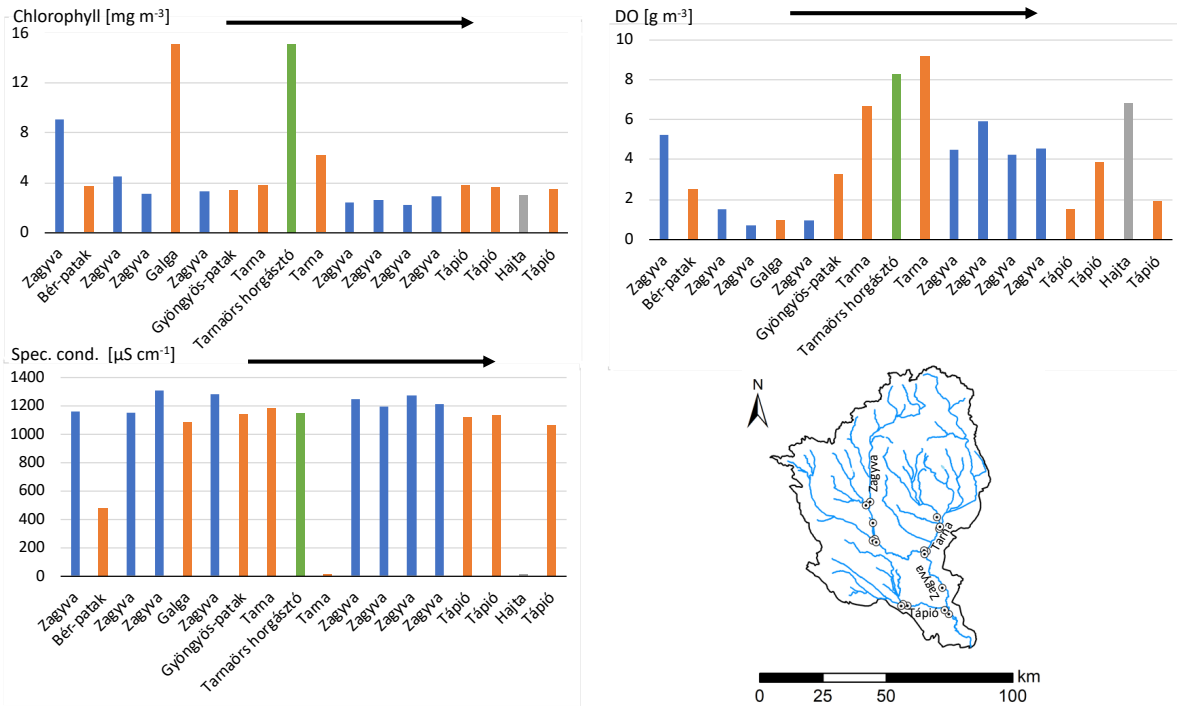


Figure 3: Concentration of chlorophyll *a* and dissolved oxygen (DO), specific conductivity (Spec. cond.) on 1 September 2020 in the Zagyva River network. (Sampling sites are shown in the map. Arrows indicate flow direction along the main river. Blue – the Zagyva River. Orange – first-order tributaries of the Zagyva River. Gray – first-order tributary of the Tápió Creek. Green – fishpond on the Tarna River.)

Flow was very low during our visit: $1.1 \text{ m}^3 \text{ s}^{-1}$ and $1.6 \text{ m}^3 \text{ s}^{-1}$ at the Tarna River mouth and in the Zagyva River upstream of the Tarna, respectively (mean flows are 4 and $5.6 \text{ m}^3 \text{ s}^{-1}$, respectively). The chlorophyll profile along the Zagyva was anomalous but typical for this river (Istvánovics and Honti, 2012): the highest concentration was recorded at the most upstream site visited. This pattern is due to the numerous eutrophic upstream reservoirs and fishponds (Erős et al., 2011) that release phytoplankton into the river. In our measurements, this could be seen as the difference between the chlorophyll concentration in the Tarna River upstream and downstream of the Tarnaörs fishpond. The impact of tributaries on the main river was modest because of the small tributary discharges and material fluxes.

Regular water quality samplings along the Rába and Zala Rivers (45 and 41 samples, respectively) indicated that the sampling strategy based on network topology was superior in comparison to the traditional sampling strategy that aims at capturing water quality profiles along an important main river without sampling at least major tributaries and standing water bodies (Fig. 4). Without catchment modelling, the reasons for the irregularities of these profiles cannot be understood. The mean chlorophyll profiles correctly reflect that phytoplankton biomass does not increase monotonically along a river as it might be expected if water residence time and resource availability were the only determinants of biomass. Irregularities are primarily due to the topographic structure of the river network graph as we saw it in the example of the Zagyva River (Fig. 3). At the same time the order of magnitude higher biomass in the much larger Rába River compared to the small Zala River (mean flows are 27 and 6 m³ s⁻¹, respectively) is clearly indicative of the fundamental role of water residence time/flushing in phytoplankton growth in rivers.

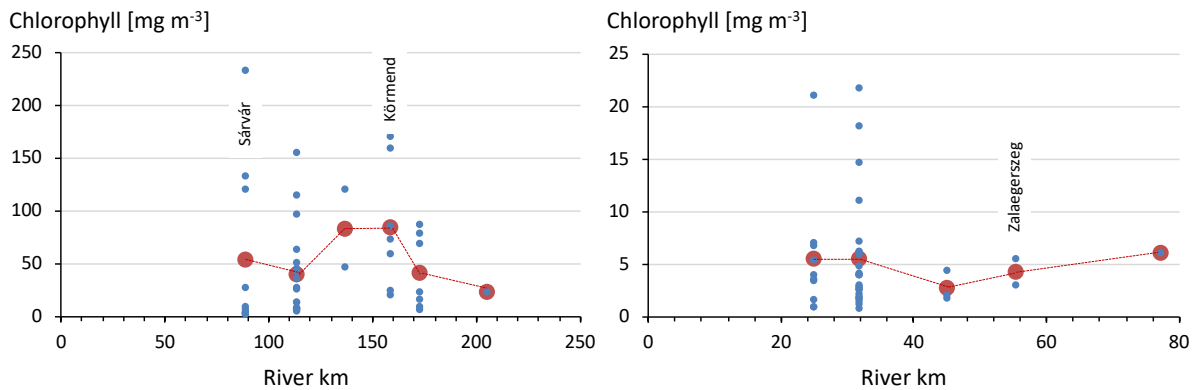


Figure 4: Concentration of chlorophyll a along the Rába (left) and Zala (right) Rivers. (Samples were taken between May-October 2019-2021. Blue circle: Individual data. Red circle: average values. Positions of largest riverbank towns are indicated by their names. In the Zala River, distance is measured from the Kis-Balaton Reservoirs.)

River Basin Management Plans of the Zagyva and Tarna Rivers indicated that zero and 2 out of the 17 and 26 river water bodies, respectively had good ecological status according to the qualification of the EU Water Framework Directive (KTVI 2016, ÉMVI 2016). Accordingly, we found that hypoxia (dissolved oxygen < 1 g O₂ m⁻³) was characteristic along a nearly 50 km long stretch of the Zagyva River downstream of the town of Hatvan (capacity of the WWTP discharging into the Zagyva is 4,900 m³ d⁻¹) and upstream of the Tarna River. Oxygen saturation approached 100% only in the Tarna River and the sampled fishpond. Specific

conductivity was below $500 \mu\text{S cm}^{-1}$ only in the Bér Creek, while values recorded elsewhere were higher by a factor of 2 to 2.5. Both the increase in conductivity and the decrease in oxygen concentration were indicative of overloading of the river network with (treated) sewage. The broad agreement between the results of our sampling expeditions and the labor-intensive EU WFD (2000/60/EC) compatible qualification suggests a possibility to rationalize the latter system. The suggested procedure would consist of two hierarchical assessment steps. First, *in situ* measurements should be taken during the vegetation period (preferably between early June to late September) on the basis of network topology similar to our sampling strategy. River water bodies, in which the morning oxygen concentration is below $2\text{--}3 \text{ g m}^{-3}$ or specific conductivity exceeds the values associated with catchment geochemistry (as measured in a number of 1st and 2nd order streams) by a factor of 2 at any time, would safely be qualified as being in less than good ecological status. In these water bodies there is no need to monitor the biotic components, it is sufficient to determine the chemical status to find the pressures responsible for the ecological deterioration. Second, ecological status of river water bodies that have more favorable oxygen and conductivity conditions than the first group should be assessed according to the present requirements of the WFD. This hierarchical system might help to economically increase spatial coverage and/or frequency of data collection in river networks without any great loss of information – a recognized need when modifying the present WFD monitoring system (Carvalho et al., 2019). Additionally, the suggested assessment procedure would introduce network thinking into the WFD that presently is missing with respect to water quality.

In early June 2022, we carried out field measurement campaigns in the Ipoly, Rába and Zala Rivers together with the Turkish Partner. Measurements with the EXO2 sonde were supplemented with spectroradiometric measurements and water sampling. Processing of these datasets will be presented in section 2.1.

2. MODELLING

2.1. Use of remote sensing in river water quality assessment

The Turkish Partner aimed at finding relationships between water quality data, spectroradiometric data and LANDSAT-7 imagery with the perspective of applying Earth

observation data for river water quality assessment. This effort has relevance for future development of the WDF monitoring system (Carvalho et al., 2019) and for efficient and economically feasible water quality monitoring in large countries such as Turkey, in data-poor environments such as many developing countries, and in transboundary rivers such as the Danube.

The methodology (Fig. 5) has been developed for processing similar data sets obtained in the 3 Turkish study rivers (Ulus, Melendiz and Firtina sampled at 85, 55 and 62 sites, respectively) during this project. Since the Hungarian lowland rivers (Ipoly, Rába and Zala) are more eutrophic than the steep, high-altitude Turkish rivers, the method could further be developed using the data of our joint Hungarian expedition. Three major improvements were made: 1) the model was jointly optimized for the five trophic response variables via artificial neural networks (ANN), 2) multiple linear regressions were replaced by generalized regression models with an adaptive elastic-net estimation method, and 3) the relationship between spectroradiometric and LANDSAT data was explored by multiple non-linear regression models.

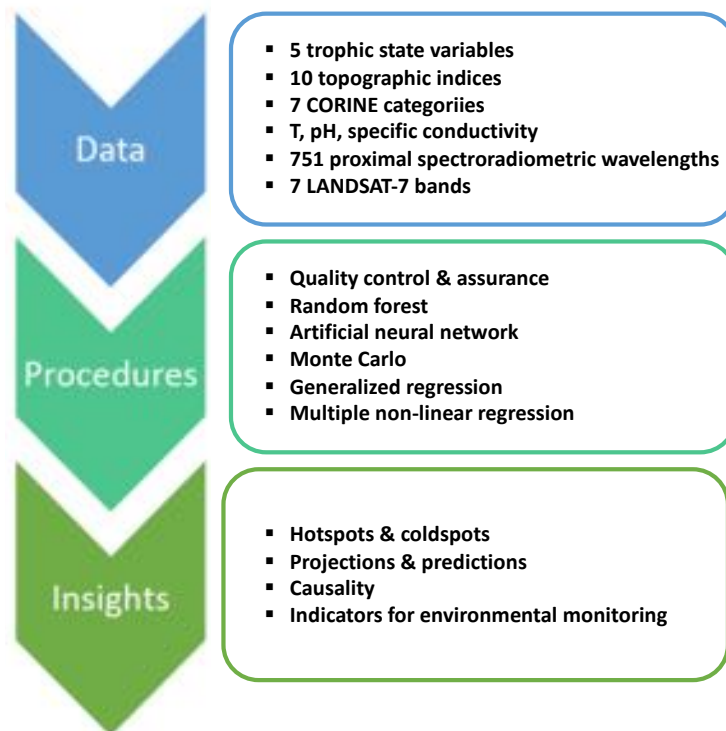


Figure 5: Work flow of the river water assessment model based on remote sensing.

Turbidity [FNU], chlorophyll *a* fluorescence [RFU], and concentrations of dissolved oxygen [DO, g O₂ m⁻³], total nitrogen [TN, mg m⁻³] and total phosphorus [TP, mg m⁻³] were considered as trophic state variables. Explanatory variables included geographical position of the sampling sites (latitude [LAT], longitude [LONG]), local and catchment-scale topological features of the study rivers derived from the SAGA GIS application (<https://sagatutorials.wordpress.com/basic-terrain-analysis/>), CORINE 2018 land use/land cover categories (<https://land.copernicus.eu/pan-european/corine-land-cover/clc2018>), background physico-chemical variables (water temperature [T, °C], pH, and specific conductivity [SC, μS cm⁻¹] and remote sensing data. The topological indices included DEM (digital elevation model), hill shading, valley depth, local morphometric terrain parameters (slope, aspect, slope length) catchment area, channel network base level, channel network distance, topographic wetness index. Remote sensing data were obtained 1) with a hand-held spectroradiometer that took reflectance spectra (ρ) at 751 proximal sensor wavelengths (W) in the 325-1075 nm range and 2) by downloading LANDSAT-7 digital number (DN) data closest in time to the field measurements.

As a quality control/quality assurance procedure, outliers beyond 3 times the interquartile range were removed from the dataset. Thereafter, we reduced the number of W s to be included into the regression models by selecting the 5 most important W s. For this purpose, random forest models with 5-fold cross-validation and the ANN algorithm with bootstrapping were used. The ANN had one hidden layer with 3 neurons, hyperbolic tangent activation function, and a learning rate of 0.1. Performance indicators (maximum predictive power [R^2] and minimum RMSE) showed that ANN models outperformed the random forest models. The 5 most important W s were selected from the best-fit ANN model. The relative importance of these W s, including both the main and interaction effects, was quantified by Monte Carlo resampling. The maximum and minimum R^2 values were obtained for the chlorophyll concentration (0.85) and turbidity (0.45), respectively. The relative importance of spectroradiometric wavelengths was as follows: $W_{465} > W_{654} > W_{372} > W_{340} > W_{1049}$. Of these, the two most important W s were in the range of in vivo absorption spectra of chlorophyll pigments while the importance of the two ultraviolet wavelengths might be associated with the presence of colored dissolved organic matter not measured in the study rivers.

Next, generalized regression (GR) and ANN models were used to predict the 5 trophic response variables from all of the predictor variables except LANDSAT data. Prior to the analysis, normality and lack of autocorrelation were checked by the Anderson-Darling and the Durbin-Watson tests, respectively. No mathematical transformation of the data was necessary. The variance inflation factor of the GR models was below 10 for each explanatory variable, indicating the absence of a multi-collinearity issue. In addition to the above performance indicators (R^2 and RMSE), the Akaike Information Criterion for small sample size (AICc) was also used to select the best GR model (Table 1). With the exception of TP, pH was a powerful predictor in each model. Other predictors occurring in 2 or 3 models were water temperature, latitude, W_{1049} and land use.

Table 1: Performance indicators of the generalized regression models. (N – sample size; n – number of predictor variables in the best model).

N	Response variable	AICc	RMSE	R^2	n
21	DO [$\text{g O}_2 \text{ m}^{-3}$]	31.0	0.39	0.90	2
17	Turbidity [FNU]	200.2	55.4	0.60	3
21	Chlorophyll [RFU]	91.7	1.25	0.91	5
21	TN [mg N m^{-3}]	23.4	0.21	0.94	6
21	TP [mg P m^{-3}]	-63.7	0.03	0.73	3

ANN models were used to jointly predict the 5 trophic state variables. The predictive power decreased in the order: TN > TP > Chl a > DO > turbidity. Regardless of the objective function (maximization, minimization, or average), the 5 most influential predictors were pH > CORINE land use > valley depth > latitude > specific conductivity. Thus, both the GR and ANN models consistently pointed to pH as the most important explanatory variable of the trophic state indicators.

Finally, linear and non-linear relationships between the reflectance at the 5 most important spectroradiometric W_s and LANDSAT-7 DN data were examined using multiple non-linear regression (MNL) models with the perspective of replacing spectroradiometric data with satellite imagery. Landsat-7 DN data were the median values in a 3×3 pixels window. Prior to setting up the models, multi-collinearity was tested. The highest correlation coefficient ($r =$

0.76) was found between reflectance at W_{465} and W_{372} , but even this value was lower than 0.8, that is the threshold coefficient, often suggested to indicate a multi-collinearity problem to be addressed. No multi-collinearity issue existed between bands 3 and 5 ($r = 0.46$); bands 3 and 1 ($r = 0.80$), and bands 1 and 5 ($r = 0.15$). The 3 most important LANDSAT-7 bands were 3 > 5 > 1 (630-690 nm [red], 1550-1750 nm [shortwave infrared] and 450-520 nm [blue], respectively). The highest Spearman's correlation coefficients (r) were found between LANDSAT band 3 and either reflectance at W_{465} ($r = 0.65$, $p < 0.001$) or W_{654} ($r = 0.64$, $p < 0.001$). For these W s, the predictive power (R^2_{pred}) of the best-fit MNLR models based on cross-validation was 0.88 and 0.83, respectively. The relatively high R^2_{pred} values suggested that application of satellite data was a promising tool for large-scale water quality assessment in rivers, too.

The Hungarian Partner also explored the potential of Earth observation data (SENTINEL-2 imagery) in trophic status assessment of rivers. Our field visits suggested that the study rivers might be too narrow during most of their course to be visible in satellite images without interference from the riverside vegetation. Nevertheless, we focused on the outflow section of the Zala River into the Kis-Balaton Reservoirs, where the river passes in a wide meadow (no shading by trees), the channel is relatively free of aquatic macrophytes, and long-term daily to weekly water quality measurements were available from the West Transdanubian Water Directorate. The SENTINEL-2 revisits Hungary every 5 days, but several images had to be discarded due to heavy cloudiness. In the period August 2015 and October 2021, 208 atmospherically corrected reflectance sets were found for the lower Zala River – Kis-Balaton – Balaton West region. Despite the exceptionally frequent long-term water quality monitoring, there were only 35 cases where field measurements (chlorophyll [mg m^{-3}], suspended solids [g m^{-3}], and UV extinction [cm^{-1}]) and satellite images could be paired with only a ± 1 day difference. Thanks to the long-term water quality data set, ranges of the variables were relatively wide (chlorophyll: 2.5 to 25 mg m^{-3} ; suspended solids 9 to 616 g m^{-3} ; UV extinction 0.098 to 0.431) to use the calibrated models during most environmental conditions occurring in the examined region.

Readily available chlorophyll models performed badly due to the optical complexity of the shallow river water. Therefore, we developed new models to jointly estimate concentration

of chlorophyll and suspended solids from reflectance data detected in the 12 wavelength channels of SENTINEL-2. The random forest method was unsuitable: it predicted over 10% negative values even for the training set. While ANN models with 3 hidden neurons provided a good fit to chlorophyll and suspended solids both in the open water areas of the Kis-Balaton Reservoirs and in Basin 1 of Lake Balaton ($0.96 < R^2_{\text{pred}} < 0.99$), the Zala River has indeed proved too narrow to reliably analyze its water quality using satellite data. Although not planned in the present project, the ANN lake models can be considered as an important project outcome that allows us to follow spatial development of algal blooms in Lake Balaton and in its pre-reservoir (the Kis-Balaton).

2.2. Application of the PhosFate-TAPIR model to the study rivers

Details of the PhosFate-TAPIR catchment-scale steady-state eutrophication model has been published (Honti et al., 2010; Istvánovics et al., 2014); we outline only the modifications introduced in the present project. After setting up the PhosFate model (Kovács et al. 2008), the TAPIR model was completely reimplemented within the PhosFate modeling environment to run the model simultaneously for each Hungarian catchment. The PhosFate model estimated discharge and diffuse phosphorus (P) loads for the whole river network acceptably. Algal growth was simulated with the TAPIR model, which calculated the biomass of both fluvial and lacustrine algae as a function of P concentration, water residence time and specific adaptation strategies of the two algal groups.

A comprehensive GIS database was created for the 5 Hungarian study rivers (Rába, Zala, Kapos, Zagyva, Ipoly; <http://ecology.vit.bme.hu/mark/GIS/>). Our model needs a series of GIS, meteorological, statistical and water quality data. The following maps were downloaded, converted to the EPSG:23700 – HD/EOV projection system and intersected with the catchment boundaries:

- Digital elevation model: EU-DEM (<https://www.eea.europa.eu/data-and-maps/data/copernicus-land-monitoring-service-eu-dem>)
- Land use: CORINE Landcover 2018 (<https://land.copernicus.eu/pan-european/corine-land-cover/clc2018>); the 51 land use categories were re-classified into 17 categories.

- Physical soil properties: European Soil Database (<https://esdac.jrc.ec.europa.eu/resource-type/european-soil-database-soil-properties>)
- Catchment and stream network: European Catchment Database (JRC CCM2, <https://ccm.jrc.ec.europa.eu>)
- Location and surface area of standing waterbodies: OpenStreetMap (<https://www.openstreetmap.org>).

Meteorology data included daily precipitation, air temperature and wind time series for the period 2009-2019. These data were obtained from the Hungarian Meteorological Service, from the National Oceanic and Atmospheric Administration (USA) and from the Digital Atlas of the Federal State of Steiermark (Austria). The finest and lowest spatial resolution was characteristic of the upper Rába catchment (Austria; e.g. precipitation was recorded at 153 sites, equivalent to 1 site per 22 km²), and the upper Ipoly catchment (Slovakia, where only 2 meteorological observatories are found, equivalent to 1 site per 1,825 km²). Daily data were averaged for the summer and winter half-years and 100x100 m resolution maps of these variables were constructed. Summer precipitation was estimated by a multivariate linear regression model considering elevation (Z) and easting (the EOY Y coordinate; $r^2=0.86$, $P<0.001$, standard error = 44 mm). Residuals of the regression were interpolated by kriging using the location of the precipitation gauges. Maps of winter and summer temperatures were based on univariate linear regression since Z alone sufficiently described spatial distribution of data ($r^2=0.86$ in summer, $r^2=0.75$ in winter). For the winter precipitation, the multivariate regression performed poorly ($r^2=0.22$). Therefore, measured values were directly interpolated. Wind maps were also constructed with direct interpolation of measured values.

Statistical and water quality data were taken from the 2nd River Basin Management Plans (2015; <https://vizeink.hu>) of the study rivers. In spite of the numerous country-specific differences in the compilation of RBMPs, we combined the Austrian and Slovakian data with the Hungarian ones for the Rába and the Ipoly Rivers, respectively. Daily mean water discharges (2001-2016) were collected from diverse sources. We found data for 69 gauges in the Rába catchment representing 33 watercourses; 39 gauges in the Ipoly catchment representing 23 watercourses; 13 gauges in the Kapos catchment representing 8 watercourses; 9 gauges in the Zala catchment representing 5 watercourses, and 11 gauges in

the Zagyva catchment representing 5 watercourses. Daily data were averaged for the summer and winter half-years.

Growth parameters of the two algal groups were set to the values established for the Szamos River network (Istvánovics et al. 2014). Simulated discharges and chlorophyll concentrations fell into the right order of magnitude for each study river. Of the 5 rivers, the Zagyva River was the most eutrophic owing to the abundant nutrient supply and long water residence time, which provided ample time to exploit the available resources. Of the 2808 ponds and reservoirs situated in the catchments of the 5 rivers (estimated volume $>1000 \text{ m}^3$), phytoplankton could be P limited only in a few dozens of water bodies. The land use optimization module of the PhosFate model assigned the upstream catchments of non-P limited standing waters to Algal Management Zones (AMZ), in which reduction of diffuse P loads may reduce algal biomass in both the standing water bodies and the downstream reaches of the recipient streams (Figs. 6-8).

Algal Management Zones covered the largest proportion in the Kapos catchment, where the entire catchment of the Koppány Creek and most of the other northern tributaries of the Kapos River fell into this category. However, even a successful AMZ nutrient management would not significantly improve the trophic status of the lower Kapos River, since fluvial algae grow in large quantities in the river.

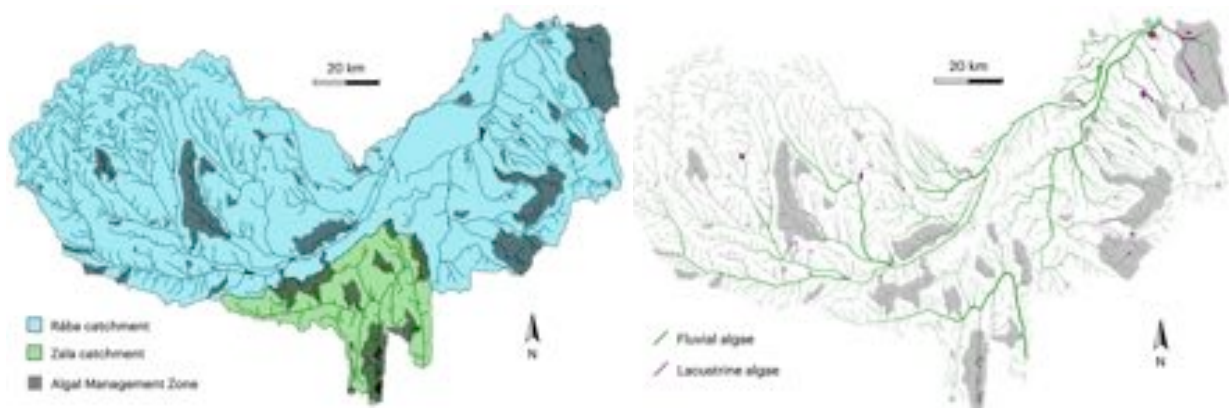


Figure 6: Algal Management Zones in the Rába and Zala catchments (left) and calculated concentrations of fluvial and lacustrine algae (right). (Line width is proportional to concentration.)

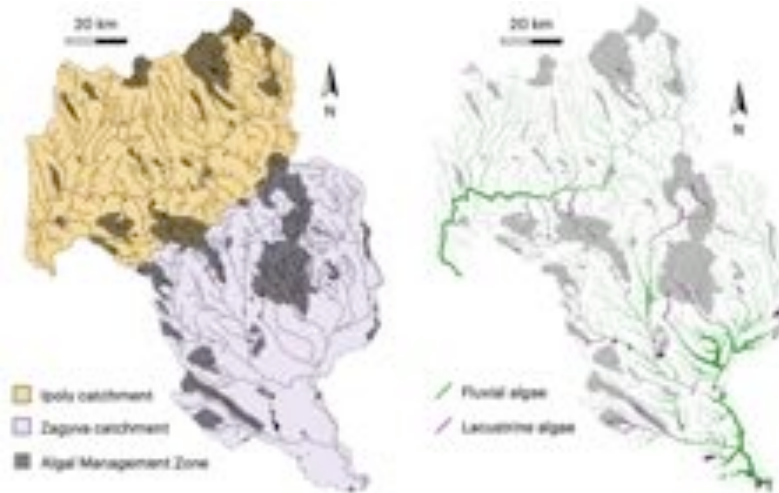


Figure 7: Algal Management Zones in the Ipoly and Zagyva catchments (left) and calculated concentrations of fluvial and lacustrine algae (right). (Line width is proportional to concentration.)

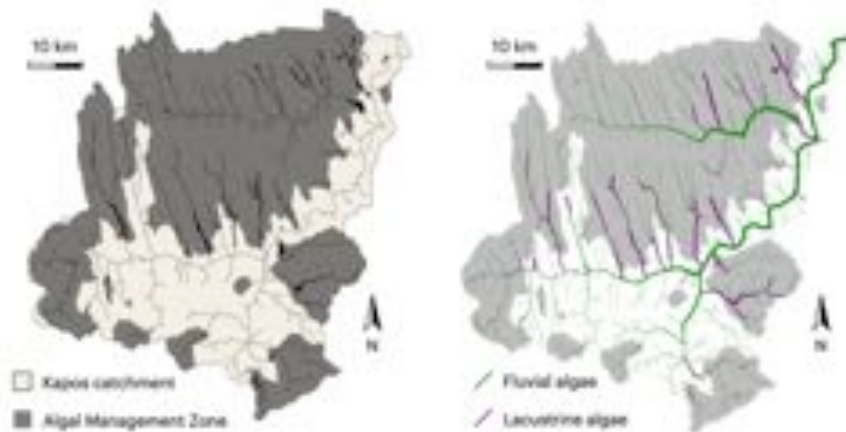


Figure 8: Algal Management Zones in the Kapos catchments (left) and calculated concentrations of fluvial and lacustrine algae (right). (Line width is proportional to concentration.)

The PhosFate model was also run for the Ulusu and Melendiz Rivers with the same settings as for the Hungarian ones. The complex topography of the Turkish catchments would have required high spatial resolution long-term meteorological data, which, however, were not available. Therefore, we used weather data from the WorldClim global database (<https://worldclim.org>). We could not obtain soil data for the study areas. Therefore, we assumed a mixed physical texture (silt) across the whole catchments and used the land use-specific mean humus and P content characteristic for the Hungarian study rivers. Maps were converted to the ETRS89 Lambert Azimutal Equal Area metric projection system.

Unlike the lowland Hungarian rivers, the Turkish rivers were not prone to eutrophication. The mountainous Ulusu catchment has a compact shape and the stream network is composed of

several branches that join only in the vicinity of the outflow (Fig. 9). These network topology points toward a short water residence time, which together with the low number of standing water bodies prevent the growth of both fluvial and lacustrine algae. The Melendiz catchment is situated in a high-altitude, arid region. Very low summer flows prolonged the residence time of algae in the stream, especially in the upstream basin around Divarlı and Çiftlik. Yet, again due to the lack of standing water bodies and the steep channel, the longest travel time in the system was about 9.5 hours, too short for the production of a substantial algal biomass.

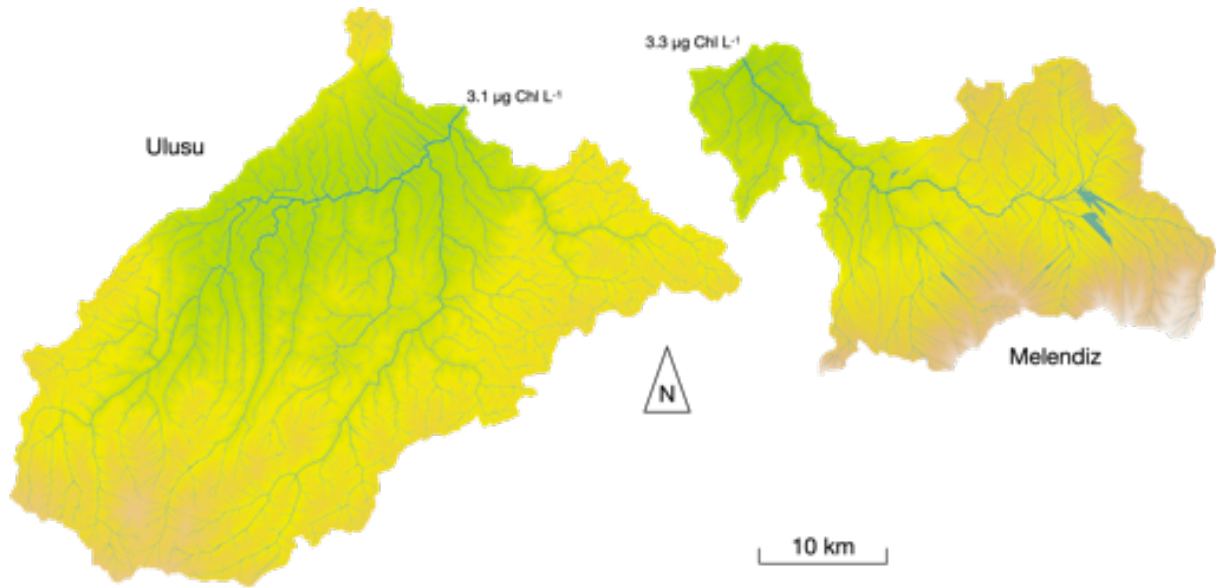


Figure 9: Simulated algal biomass in the stream networks of the Ulusu (left) and Melendiz (right) Rivers. (The mean chlorophyll concentration in the outflow is shown.)

The Turkish Partner made efforts to apply the MapShed watershed modelling tool (<https://www.midatlanticrisa.org/data-tools/water-model-tool/items/mapshed.html>) to the Ulusu and Zala Rivers. The considerable data requirement of this dynamic model, however, could not be satisfied to achieve an acceptable performance.

2.3. Developing a simplified conceptual stream network eutrophication model

A major conclusion from the above modelling exercise was that even steady-state catchment-scale models of river eutrophication, like the PhosFate-TAPIR model, require large amounts of data, not to mention dynamic models, like MapShed. It is difficult to satisfy these requirements even in relatively data-rich regions such as the EU, where a significant portion of the various types of data are collected in a standardized way. At the same time,

eutrophication is still the leading global water quality deterioration issue (Downing, 2014; Jenny et al., 2020), which is expected to become even more acute due to agricultural intensification (Tschardt et al., 2012) and the impact of climate change (Dokulil et al., 2010; Meerhoff et al., 2022). Since eutrophication of river networks can efficiently be managed only at the basin scale, the need for basin scale river eutrophication models will also increase. Considering that in vast areas collection of the required data is poor or non-existing, data collected internally in a country are not easily available, and 153 countries have territory within at least one of the 286 transboundary river and lake basins that comprise 60% of the world's freshwater flows (<https://www.unwater.org/water-facts/transboundary-waters>), it is unlikely that the existing catchment-scale river eutrophication models will actually be used to plan river management at a basin scale. Although not planned in the present project, these considerations led us to develop a novel, simplified network eutrophication model that targets to approximately quantify eutrophication potential in large rivers. The model focuses only on the most important drivers of stream eutrophication and its data requirements can be covered from online databases. A case study was elaborated for the Danube Basin.

Although enhanced nutrient availability is a prerequisite of river eutrophication, there is usually no direct relationship between nutrient concentrations and algal biomass due to the basically unidirectional transport and network topology (Fig. 10; Wehr and Descy, 1998; Istvánovics and Honti, 2012). Nutrient concentrations have key importance with respect to eutrophication in the recipient standing waters and are often used as an index of eutrophication in rivers as well (Van Nieuwenhuysse and Jones, 1996; Dodds, 2006), but they do not properly characterize river eutrophication. The proper measure of the latter is only algal biomass.

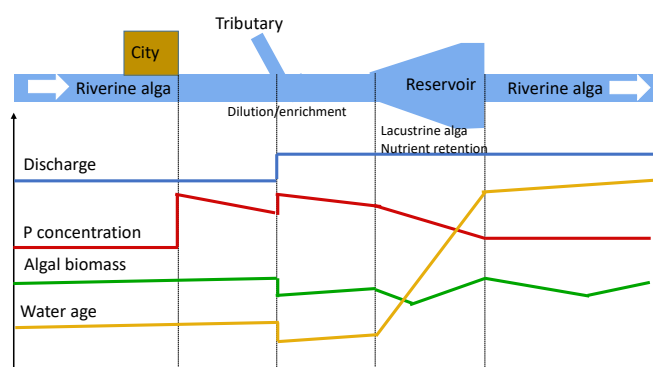


Figure 10: Discharge, phosphorus concentration, chlorophyll concentration, and water age profiles along a schematic river stretch.

Proliferation of phytoplankton in streams requires the coincidence of three independent factors: adequately high nutrient supply, an inoculum of algae from the upstream environment, and a suitable downstream hydromorphology that provides sufficiently long time for algal growth. Standing water bodies in the stream network are unsuitable habitats for fluvial algae, since they select for species that favor warmer and less turbulent waters. In this way they disrupt the continuity of phytoplankton development along the flow. In contrast, lacustrine algae washed out into the streams may temporarily determine the trophic status of the downstream network while they get slowly lost in the turbulent river environment. True riverine algae are meroplanktonic, they are adapted to the turbulent conditions of rivers. They avoid washout by spending most of their life cycle settled to the bottom in shallow areas of the riverbed (Stoyneva, 1994; Istvánovics and Honti, 2011; Istvánovics et al., 2014). Meroplanktonic algae are lost in the reservoirs. Based on these considerations, the essential features of our simple and flexible conceptual stream network eutrophication model are that it explicitly takes into consideration network topology and river continuity/discontinuity with respect to algal growth through including lacustrine and riverine (meroplanktonic) algae.

2.3.1. Methods

Table 2: Data sources

TYPE OF DATA	DATABASE	SOURCE
River network	JRC CCM2	https://data.jrc.ec.europa.eu/dataset/fe1878e8-7541-4c66-8453-afdae7469221
Lakes, reservoirs	OpenStreetMap	https://www.openstreetmap.org/
Land use	CORINE 2018	https://land.copernicus.eu/pan-european/corine-land-cover/clc2018
	& GLC	https://www.eea.europa.eu/data-and-maps/data/global-land-cover-2000-europe
Precipitation, potential evapotranspiration	WorldClim	https://worldclim.org/
Population	EUROSTAT	https://ec.europa.eu/eurostat/web/gisco/geodata/reference-data/grids
Population UA, MD	Wikipedia	
Discharge	GRDC	https://grdc.bafg.de
Concentration of chlorophyll <i>a</i>	TNMN	https://www.icpdr.org/main/activities-projects/tnmn-transnational-monitoring-network

Besides the stream network, the JRC CCM2 database (Table 2) provides basic information for stream sections, such as local catchment area, length, mean channel slope. Sub-catchment areas vary in size from 0.01 to 177 km²; all of the other maps were rescaled to the variable scale of CCM2. Standing waters from the OpenStreetMap and monitoring sites were assigned to stream sections based on name/position.

The model consists of three modules (Fig. 11): a hydrology and hydraulic module, a nutrient load module and an algal growth module. The combination of topological, hydrological and hydraulic factors determines whether an increase in nutrient loading in a given watercourse will or will not cause eutrophication. In other words, this module of the model estimates the susceptibility (vulnerability) of rivers to eutrophication.

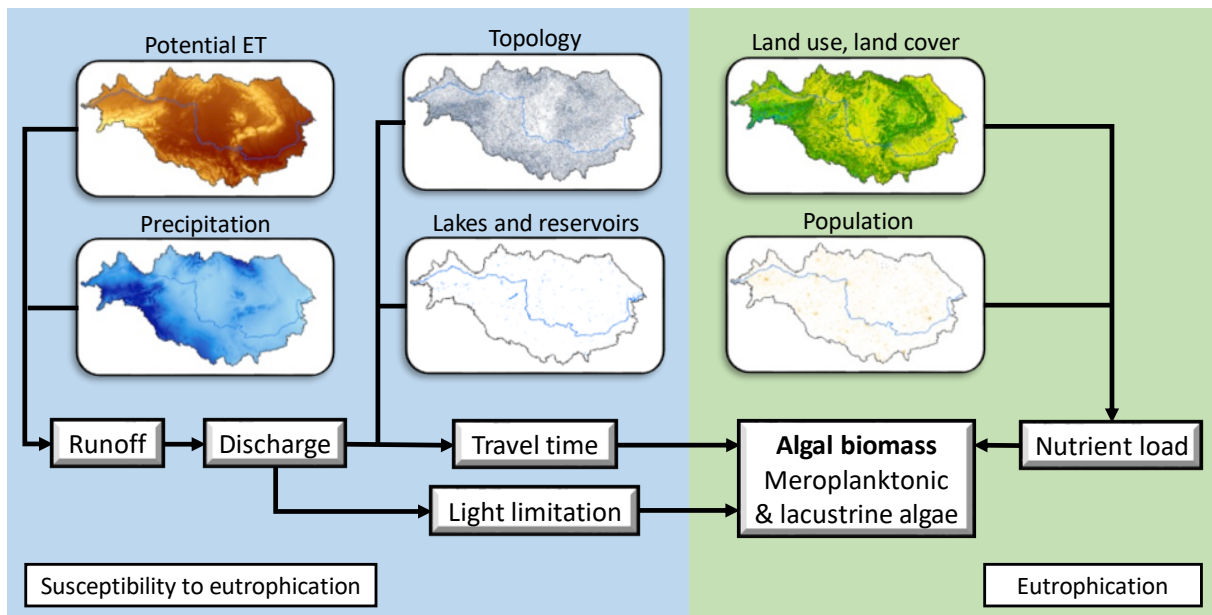


Figure 11: Structure of the simplified river network eutrophication model.

Mean annual runoff (q , [mm]) was estimated by the adjusted empirical function of Berkaloff and Tixéront (1958):

$$q = \frac{P^3}{4.8 PET^2},$$

where P is annual precipitation [mm] and PET is potential evapotranspiration [mm]. Runoff was converted into local discharge by multiplying q with the local catchment area. Local discharge was accumulated into total discharge (Q , [m³ s⁻¹]) along the network.

Mean flow velocity (v , m s^{-1}) was calculated by the Manning (1891) equation assuming a channel roughness of 0.04 m. To use this equation, first we had to estimate channel width (W , [m]) and depth (D , [m]). The $W:D$ ratio (α [-]) was estimated from channel slope (S [-]) as

$$\alpha = 4 (S)^{-1/2}$$

based on the observation that finer bed material, which usually occurs at gentle slopes tend to coincide with larger relative width or lower relative depth (Finnegan et al.; 2005). Knowing the discharge, the depth needed to convey the flow was expressed as

$$D = \left(\frac{\left(\frac{\alpha}{\alpha + 2} \right)^{1/3} (\alpha + 2) n Q}{\alpha^2 \sqrt{S}} \right)^{3/8}$$

The width, hydraulic radius (R [m]) of the cross-section and flow velocity are as follows:

$$\begin{aligned} W &= \alpha D \\ R &= \frac{D W}{W + 2 D} \\ v &= R^{2/3} \frac{\sqrt{S}}{n} \end{aligned}$$

Where not known, volume of lowland (altitude ≤ 700 m) and high-altitude (>700 m) lakes and reservoirs was taken as 3.25 and 25 m, respectively. Water residence time (τ , [d]) was calculated from channel length and flow velocity in stream sections, and from volume and discharge in standing water bodies. Mean water age was calculated by discharge-weighted accumulation of τ .

The CORINE land cover classification was simplified into 6 categories (Table 3). Effective area-specific nutrient emissions were assigned to land use classes based on mean values from previous Central-European applications of the PhosFate model (Kovács et al., 2008; Honti et al., 2010; Istvánovics et al. 2014). Daily per capita human emission was assumed to be 2 g P. P removal efficiency at WWTPs was set to 90% in Germany, 70% in Austria, 0% in Moldova, Ukraine, and Serbia, and 30% elsewhere. P from WWTPs was considered to be dissolved. P retention was neglected in watercourses and estimated in lakes and reservoirs by the OECD (1982) model.

Table 3: Reclassified CORINE land use categories and their effective area-specific nutrient emissions.

Category	Description	Area-specific effective diffuse dissolved P emission [mg P m ⁻² yr ⁻¹]
URBAN	Impermeable surfaces of settlements with P emissions from population or traffic	52.27
ERODABLE	Arable land and areas with durable exposure of bare soil surface	1.40
WOODY	Tree-covered areas, such as forests	0.13
SHRUB	Bush-covered areas, pastures, orchards, etc.	0.63
INERT	Non-urban impermeable surfaces	51.81
WATER	Wetlands	11.47

Two groups of algae were distinguished: lacustrine and riverine (meroplanktonic) algae. Each first order stream was inoculated with both types of algae in an initial chlorophyll concentration of 1 mg m⁻³. Growth and mortality of the two algal groups were dependent on habitat type, residence time, P concentration and light conditions. Habitats were identified as lakes if the water residence time exceeded 1 day and as rivers if it was shorter. We assumed that algae grew and decayed at the same net rate in- and outside of their preferred habitat. The rates were set to $k=\pm 0.2 \text{ d}^{-1}$ for riverine and $k=0.25 \text{ d}^{-1}$ for lacustrine algae. We assumed that one unit of P was required to produce one unit of chlorophyll. When the available P supply was exhausted, growth stopped. Similar to previous TAPIR applications, 30% of the average dissolved P load was considered to be available for algal growth in rivers.

Meroplanktonic algae spend a fraction of their time settled on the bottom, so they travel slower downstream than the water. This means that the higher the proportion of time spent settled and floating, the higher the apparent growth rate compared to the 'real' growth rate of 0.2 d^{-1} . The expected ratio of time spent settled and in the drag of the flow was approximated by the method developed to estimate the distribution of fine sediment between the bottom and the water column (Honti et al. 2018). According to this method, the ratio is calculated from the typical suspended solids concentration in the water ($SSC \approx 30 \text{ g m}^{-3}$) and fine particle mass in the active sediment layer (M_{act} ; g m^{-2}):

$$\frac{t_{settled}}{t_{suspended}} = \frac{M_{act}}{SSC \cdot D}$$

M_{act} was found by assuming a 0.01 m active depth, 50% porosity and $2,500 \text{ kg m}^{-3}$ grain density.

Light available for floating (I_{water} ; [$\mu\text{mol m}^{-2} \text{s}^{-1}$]) and settled algae (I_{set} ; [$\mu\text{mol m}^{-2} \text{s}^{-1}$]) was identical to the illumination at the middle and at the bottom of the water column, respectively:

$$\frac{I_{water}}{I_0} = \exp\left(-k_{ext} \frac{D}{2}\right)$$

$$\frac{I_{set}}{I_0} = \exp(-k_{ext} D),$$

where I_0 [$\mu\text{mol m}^{-2} \text{s}^{-1}$] is the incident light intensity and $k_{ext} \approx 1.8 \text{ m}^{-1}$ is the coefficient of diffuse light attenuation. Relative productivity (Pr [-]) under the corresponding relative light intensity of the two states of meroplankton was calculated with the hyperbolic tangent function assuming that 10% of I_0 saturated net growth:

$$Pr_{water} = \tanh\left(10 \frac{I_{water}}{I_0}\right)$$

$$Pr_{set} = \tanh\left(10 \frac{I_{set}}{I_0}\right)$$

Thus, the actual net growth rate of meroplanktonic algae (k_{act} , [d^{-1}]) was:

$$k_{act} = k \left(Pr_{water} + Pr_{sed} \frac{t_{settled}}{t_{suspended}} \right), k_{act} \leq 12 k.$$

In shallow low order streams, meroplanktonic algae may not be present but benthic algae attached to the substrata may be abundant (Biggs, 2000). The latter equation would predict excessive actual net growth rates for benthic algae. To distinguish between meroplankton and true benthic algae, k_{act} was constrained not to exceed k by more than a factor of 12.

The baseline model was validated against long-term (roughly the past two decades) mean discharge and chlorophyll data. The validated model was used for scenario analysis to understand how nutrient emission, reservoir construction and climate change influence river eutrophication (Table 4). Scenarios 1 and 2 compared the two extremes of point source management: the complete lack of sewage treatment and the implementation of the best wastewater treatment technology across the whole Danube Basin, respectively. Scenario 3 accounted for major impacts of climate change, that is reduced precipitation, increased PET , increased water retention in reservoirs and enhanced irrigation of arable land. Scenario 4 examined the impact of modification of network topology by eliminating reservoirs.

Table 4: Scenarios implemented in the simplified river eutrophication model.

Scenario	Description
Baseline	Calibrated and validated by observed mean data
Scenario 1	No wastewater treatment anywhere.
Scenario 2	P removal efficiency is 90% in each WWTP.
Scenario 3	5% less rainfall, 5% more potential evaporation, enlarging each reservoir by 20%, water abstraction to irrigate 30% of arable land to satisfy a water demand equivalent to 700 mm yr ⁻² precipitation.
Scenario 4	No reservoirs.

2.3.2. Results and Discussion

For its simplicity, the baseline model simulated well the average discharge across the river network and reasonably reproduced the pattern of chlorophyll concentration along the flow (Fig. 12) consistently observed in the Danube River (Dokulil, 2014).

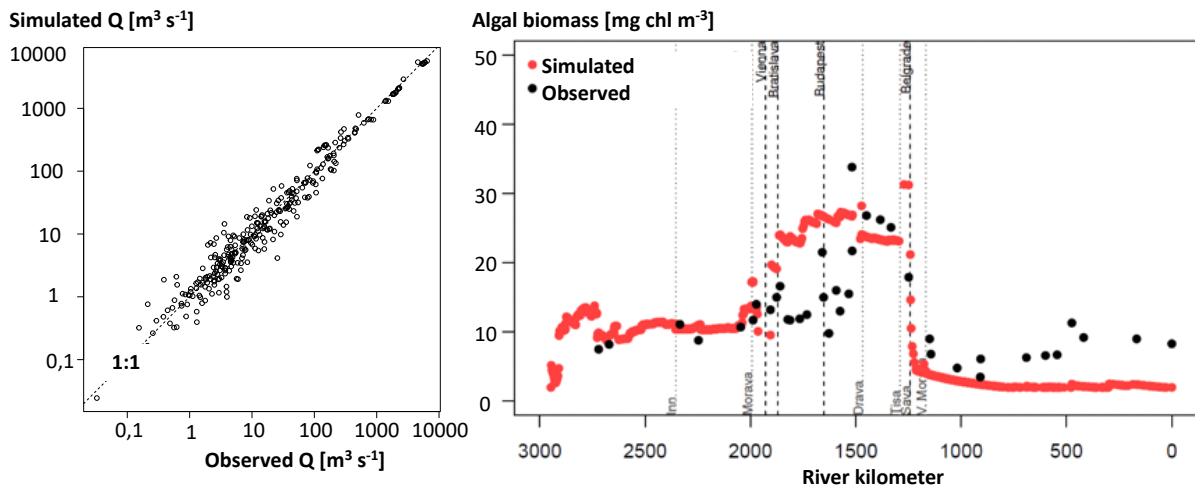


Figure 12: Comparison of measured and calculated discharge (Q, left) and algal biomass profile along the Danube River (right).

The model showed that algae started to grow immediately downstream of Vienna where channel slope decreases, water residence time increases, and nutrient availability was sufficiently high. The biomass plateaued in between Budapest and the confluence of the Tisa River. The Drava, Tisa and Sava Rivers together double the discharge in the Danube. Since these tributaries carried less algae than the Danube, the concentration of chlorophyll was reduced by dilution. The Danube channel deepens to accommodate the suddenly increased mean Q and thus, light became limiting for meroplanktonic growth. Meroplankton were unable to regenerate. This process was further amplified in the Iron Gate Reservoirs, where

besides light limitation, reduced turbulence also contributed to the loss of fluvial algae. The systematic underestimation of chlorophyll downstream of the Iron Gate was due to the lack of accounting for channel heterogeneity. We estimated channel depth from discharge that implies a uniform cross-sectional depth. The estimated depth and associated light conditions did not support meroplanktonic growth along the lower Danube. In reality, however, Stoyneva (1994) showed the role of shallows in supporting meroplankton growth along the Bulgarian section of the Danube.

Of the largest tributaries, the Tisa River and the downstream section of the Sava, Velika Morava and Prut Rivers were eutrophic, while the Inn and the Drava Rivers had a favorable trophic status (Fig. 13). This was in broad agreement with the pattern observed during the Joint Danube Surveys (Dokulil and Kaiblinger, 2008).

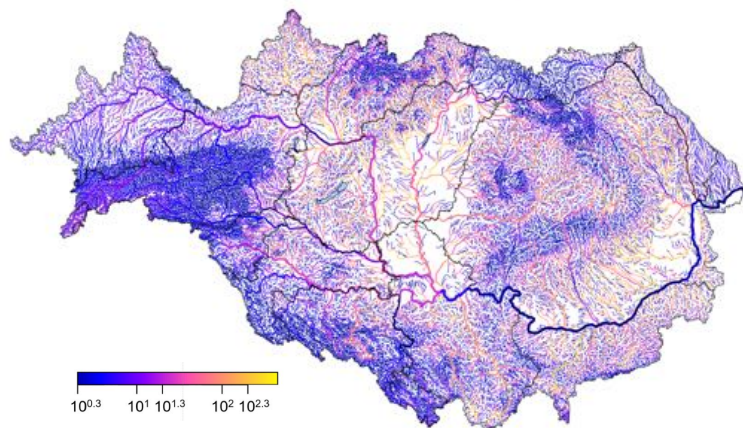


Figure 13: Distribution of simulated concentration of chlorophyll [mg m^{-3}] in the Danube River network.

In line with our previous findings (Honti et al, 2010; Istvánovics et al., 2014), spatial distribution of phytoplankton biomass indicated that large and very large lowland rivers with long free-flowing sections and without large tributaries were the most susceptible to eutrophication. Both large tributaries and reservoirs disrupted river continuity with respect to phytoplankton growth. The most conspicuous example of tributary-associated discontinuity was the collapse of phytoplankton downstream of the confluence of the Tisa and Sava Rivers within a short distance. A similarly conspicuous example is the confluence of the highly eutrophic Szamos River with the hitherto oligotrophic Tisa River that basically influences the trophic status of the whole downstream section of the main river (Fig. 13.; Honti et al., 2008;

Istvánovics et al., 2010, 2011, 2014). Reservoirs force a change in community structure selecting for species avoiding high turbulence, often including cyanobacteria and dinoflagellates (Uherkovich, 1971).

Scenario 1 indicated that efficient wastewater treatment was a major factor that maintained the favorable present trophic status of the stream network in Germany and Austria (Fig. 14). Without WWTPs, streams turned eutrophic in the upper Danube catchment with the exception of the lowest order streams. A significant trophic improvement could be achieved in the middle and lower Danube and in numerous large tributaries by introducing the best wastewater treatment technology across the whole Danube basin (Scenario 2), stressing the importance of the wastewater management initiative of the ICPDR (2021).

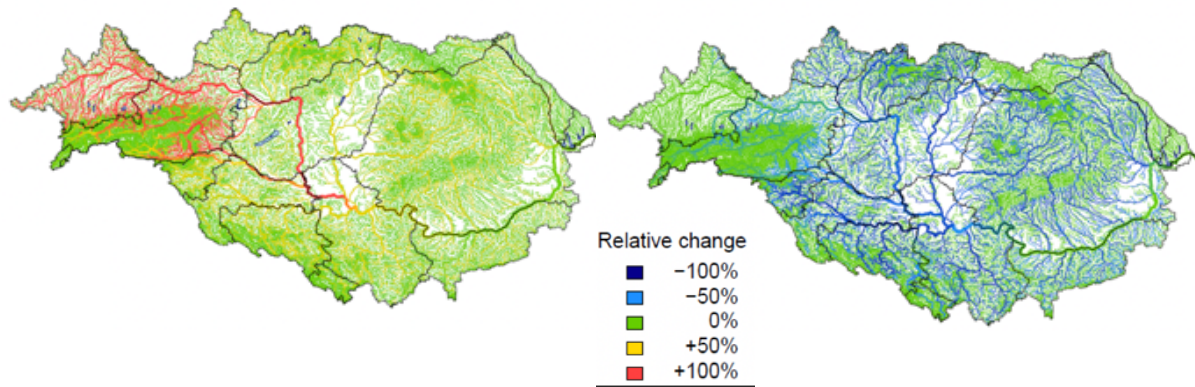


Figure 14: The relative change map of chlorophyll concentration compared to the baseline scenario when there is no wastewater treatment (Scenario 1; left) and the best treatment technology is implemented (Scenario 2; right) across the whole Danube Basin.

The climate change scenario (Scenario 3) caused a general decrease in modelled discharge (Fig. 15). This led to shallower channel depth and improved light climate, favoring meroplanktonic growth. Cumulation of the upstream changes was particularly pronounced along the lower Danube, where the biomass of phytoplankton roughly doubled.

The removal of reservoirs (Scenario 4) decreased water residence time in the river network by orders of magnitude and restored the continuity of watercourses with respect to meroplanktonic growth. The combined effect of these two factors could lead to a reduction or an increase in algal biomass in the river section downstream the removed reservoir, depending on local conditions (Fig. 16). If the reservoir was eutrophic, the biomass will

decrease along the section where lacustrine algae have decayed previously. Conversely, we may see an increase if the trophic level of the reservoir was not very high, and the dominant effect of its removal was a significant lengthening of the shallow, free-flowing section of the river, which is the optimal habitat for meroplanktonic algae.

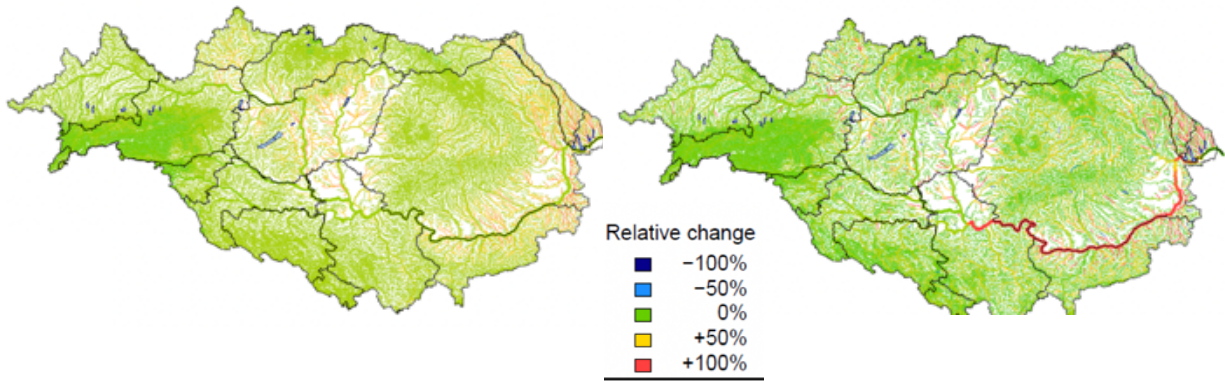


Figure 15: The relative change map of discharge (left) and chlorophyll concentration (right) under the impact of climate change (Scenario 3) compared to the baseline scenario.



Figure 16: The relative change map of chlorophyll concentration in Scenario 4 (no reservoirs) compared to the baseline scenario.

2.3.3. Conclusions

The proposed very simple model was capable of capturing the present and potential eutrophication features of the Danube at the basin scale. The model reflected the key importance of network topology and the meroplanktonic life history adaptation of fluvial algae in river eutrophication. A major benefit of holistic, basin-scale modeling was that response to management alternatives could be analyzed at a similar level. This feature is inevitable for managing large rivers, because responses often occur several 100 kilometers downstream of the site of an intervention. The model is flexible: simplified assumptions can easily be replaced by detailed and/or realistic input data and projections (e.g. wastewater

treatment, spatially distributed climate change projections, etc.) and it is applicable from river basin to continental scales.

2.3.4. Miscellaneous

A short brochure introducing the problem of river eutrophication and presenting the simplified network-scale river eutrophication model for managers has been prepared in Hungarian and English. As a step to put the model into practice, we submitted the brochure to the General Directorate of Water Management (Budapest) and to the International Commission for the Protection of the Danube River (Vienna). Feedbacks can be found in Appendix 1.

Preparation of a Q1 publication about the Danube Basin case study is in progress.

3. REFERENCES

- Berkaloff E., and J. Tixeront (1958). Notice de la carte du ruissellement annuel moyen en Tunisie. *Etudes Hydraulique et Hydrologie*, Série I, Fascicule, Vol. 7, pp. .11. BIRH, Secretariat d'Etat al'Agriculture a Tunis.
- Biggs, B. J. F. (2000). Eutrophication of streams and rivers: dissolved nutrient-chlorophyll relationships for benthic algae. *Journal of North American Benthological Society* 19: 17–31.
- Carvalho, L., E. B. Mackay, A. C. Cardoso, A. Baattrup-Pedersen, S. Birk, K. L. Blackstock, G. Borics, A. Borja, C. K. Feld, M. T. Ferreira, L. Globevnik, B. Grizzetti, S. Hendry, D. Hering, M. Kelly, S. Langaas, K. Meissner, Y. Panagopoulos, E. Penning, J. Rouillard, S. Sabater, U. Schmedtje, B. M. Spears, M. Venohr, W. van de Bund and A. L. Solheim (2019). Protecting and restoring Europe's waters: An analysis of the future development needs of the Water Framework Directive. *Science of the Total Environment* 658: 1228-1238.
- Dodds, W. K. (2006). Eutrophication and trophic state in rivers and streams. *Limnology and Oceanography* 51: 671–680.
- Dokulil, M. T. (2014). Phytoplankton of the River Danube: Composition, seasonality and long-term dynamics. In: I. Liska [ed.] *The Danube River Basin (The Handbook of Environmental Chemistry, 39)*, pp. 411-428. Springer-Verlag Berlin.
- Dokulil, M. T. and C. Kaiblinger (2008). Phytoplankton. In: I. Liška, F. Wagner, J. Slobodník [eds.] *Joint Danube Survey 2 Final Scientific Report*. ICPDR, Vienna
- Dokulil, M. T. and K. Qian (2021). Photosynthesis, carbon acquisition and primary productivity of phytoplankton: a review dedicated to *Colin Reynolds*. *Hydrobiologia* 848: 77-94.
- Dokulil, M. T., K. Teubner, A. Jagsch, U. Nickus, R. Adrian, D. Straile and J. Padisák (2010). The impact of climate change on lakes in Central Europe. In D. G. George [ed.], *The Impact of Climate Change on European Lakes*. Aquatic ecology series 4, pp. 387–409. Springer.
- Downing, J. A. (2014). Limnology and oceanography: Two estranged twins reuniting by global change. *Inland Waters* 4: 215–232.
- ÉMVI (2016). Vízgyűjtő-gazdálkodási Terv – 2015. 2-11 Tarna [in Hungarian]. p. 116. Miskolc, Hungary.
- Erős, T., D. Schmera and R. S. Shick (2011). Network thinking in riverscape conservation – A graph-based approach. *Biological Conservation* 144: 181-192.
- Honti, M., F. Bischoff, A. Moser, C. Stamm, S. Baranya, and K. Fenner (2018). Relating degradation of pharmaceutical active ingredients in a stream network to degradation in water-sediment simulation tests. *Water Resources Research* 54: 9207-9223.

- Honti M., V. Istvánovics and Á. Kovács (2010). Balancing between retention and flushing in river networks – optimizing nutrient management to improve trophic state. *Science of the Total Environment* **408**: 4712-4721.
- Honti, M., V. Istvánovics and Z. Kozma (2008). Assessing phytoplankton growth in River Tisza (Hungary). *Verhandlungen der internationale Vereinigung für theoretische und angewandte Limnologie* **30**: 87-89.
- ICPDR (2021). *Wastewater Management in the Danube River Basin*. Recommendation paper IC 242. ICPDR, Vienna
- Istvánovics, V., and M. Honti (2011). Phytoplankton growth in three rivers: The role of meroplankton and the benthic retention hypothesis. *Limnology and Oceanography* **56**: 1439-1452.
- Istvánovics, V., and M. Honti (2012). Efficiency of nutrient management in controlling eutrophication of running waters in the Middle Danube Basin. *Hydrobiologia* **686**: 55-71 (2012).
- Istvánovics, V., M. Honti, Á. Kovács, G. Kocsis and I. Stier (2014). Phytoplankton growth in relation to network topology: Time-averaged catchment-scale modelling in a large lowland river. *Freshwater Biology* **59**: 1856-1871.
- Istvánovics, V., M. Honti, L. Vörös and Z. Kozma (2010). Phytoplankton dynamics in relation to connectivity, flow dynamics and resource availability - the case of a large, lowland river, the Hungarian Tisza. *Hydrobiologia* **637**: 121–141.
- Jenny, J.-P., O. Anneville, F. Arnaud, Y. Baulaz, D. Bouffard, I. Domaizon, ... G. A. Weyhenmeyer (2020). Scientists' warning to humanity: Rapid degradation of the world's large lakes. *Journal of Great Lakes Research* **46**: 686-702.
- Kovács, Á., M. Honti and A. Clement (2008). Design of best management practice applications for diffuse phosphorus pollution using interactive GIS. *Water Science and Technology* **57**: 1727-1733.
- KTVI (2016). Vízgyűjtő-gazdálkodási Terv – 2015. 2-10 Zagyva alegység. [in Hungarian]. p.135. Szolnok, Hungary.
- Manning, R. (1891). On the flow of water in open channels and pipes. *Transactions of the Institution of Civil Engineers of Ireland* **20**: 161–207.
- Meerhoff, M., J. Audet, T. A. Davidson, L. De Meester, S. Hilt, S. Kosten, Z. Liu, N. Mazzeo, H. Paerl, M. Scheffer and E. Jeppesen (2022). Feedback between climate change and eutrophication: revisiting the allied attack concept and how to strike back. *Inland Waters* **12**: 187-204.
- OECD (1982). Eutrophication of waters. Monitoring, assessment and control. *OECD Cooperative Programme on Monitoring Inland Waters (Eutrophication control)*. Environmental Directorate, OECD, Paris.
- Stoyneva, M. P. (1994). Shallows of the lower Danube as additional sources of potamoplankton. *Hydrobiologia* **289**: 171–178.
- Tscharntke, T., Y. Clough, T. C. Wanger, L. Jackson, I. Motzke, I. Perfecto, J. Vandermeer and A. Whitbread (2012). *Biological Conservation* **151**: 53–59.
- Uherkovich, G. (1971). *A Tisza Lebegő Paránynövényei* (in Hungarian). Szolnok Megyei Múzeum Adattár, Szolnok, Hungary
- Van Nieuwenhuysse, E. E. and J. R. Jones (1996). Phosphorus-chlorophyll relationship in temperate streams and its variation with stream catchment area. *Canadian Journal of Fisheries and Aquatic Sciences* **53**: 99–105.
- Wehr, J. D. and J.-P. Descy (1998). Use of phytoplankton in large river management. *Journal of Phycology* **34**: 741-749.

4. APPENDIX 1

4.1. Response from the General Directorate of Water Management [in Hungarian]

ELKH-BME Vízgazdálkodási Kutatócsoport
Dr. Istvánovics Vera
tudományos tanácsadó részére

Tisztel Asszonyom!

Köszönettel vettük az NKFI-1 NNE 129990 szám alatt „*Folyóhálózatok eutrofizációja*” címmel elkészült nemzetközi kutatási jelentésének megküldését.

A trofitás becslét végrehajtó PhosFate modell működőképességének igazolása számunkra fontos szakmai eredmény, és a vízminőség-javító intézkedések szempontjából a foszfor limitáció igazolása a folyóvizeken is jelentős számunkra.

Mind a kutatás újszerű megközelítése, mind eredménye a gyakorlat szempontjából is igen hasznos számunkra.

Budapest, 2023. 02. 28.

Tóth György István
vízminőségi és biológus főtanácsadó

4.2. Response from the ICPDR



Dr. Vera Istvánovics

scientific advisor
project leader
ELKH-BME Water Research Group

Ref: 18692

Vienna, 16 March 2023

Letter of Recommendation

Distinguished Dr. Istvánovics,

we received the public brochure of your project that we read with great interest.

The International Commission for the Protection of the Danube River (ICPDR) welcomes the outcomes of the project, in particular the water quality model quantifying eutrophication of rivers. The development of a simple basin-wide model with limited data demand that reasonably works and is suitable to analyze management and climate change scenarios is highly appreciated.

The ICPDR will consider making use of the model for future water quality investigations in the Danube River Basin.

Moreover, we highly recommend using the model for river basin management planning at both national and transboundary level.

Sincerely,

A handwritten signature in blue ink, appearing to read 'Adam Kovacs', written over a light blue horizontal line.

Dr. Adam Kovacs

Technical Expert for Pollution Control